PERIODICA POLYTECHNICA SER. EL. ENG. VOL. 37, NO. 4, PP. 305-325 (1993)

# HARMONIC CONDITIONS OF THE CONVERTER-FED SYNCHRONOUS MACHINE

István SCHMIDT

Department of Electrical Machines
Technical University of Budapest
H-1521 Budapest, Hungary

Received: April 5, 1993

## Abstract

The operation of the converter-fed synchronous machine (CFSM) is determined by the fundamental harmonics and the mean values. The harmonics cause essentially only additional phenomena (additional losses, torque pulsation, etc.). This publication is presenting a simple method for the investigation of harmonic conditions.

*Keywords:* synchronous machine, converter, nonsinusoidal supply, current harmonics, torque harmonics, double star connection.

## 1. Introduction

The CFSM is often applied in high power speed controlled drives. In the CFSM shown in *Fig. 1* both the line-side converter (LSC) and the machine-side converter (MSC) operate with line (machine) commutation. In the motor operation of the CFSM the LSC converter works as a rectifier and the MSC converter works as an inverter, in generator operation the converters work inversely. Changing the phase sequence in the firing of MSC converter, a 4-quadrant drive can be obtained.

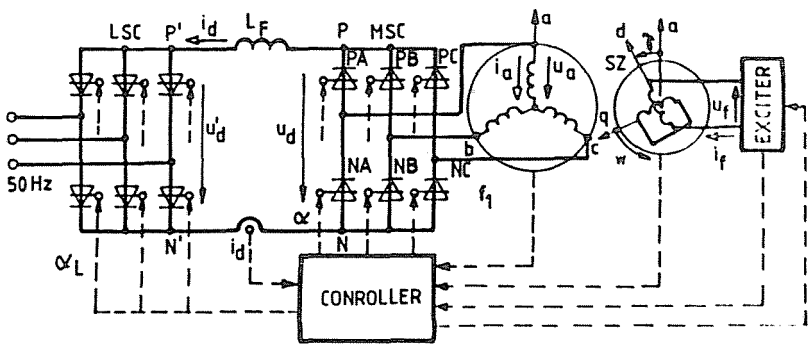


*Fig. 1.* Circuit diagram of the CFSM

## 2. The Simplified Model

We presume a synchronous machine with cylindrical rotor and of symmetric build up. Then the synchronous and subtransient inductances in the $d$ and $q$ axes are equal: $L_d = L_q$ and $L''_d = L''_q = L''$. The equivalent circuit of such a synchronous machine can be seen in *Fig. 2.* Neglecting the rotor resistances the subtransient flux $\bar{\psi}''$ and the induced subtransient voltage $\bar{u}'' = d\bar{\psi}''/dt$ consist only of a fundamental harmonic component, so in a stator reference frame their Park vectors are

$$\bar{\psi}'' = \bar{\Psi}'' e^{jW_1 t}, \quad \bar{u}'' = \bar{U}'' e^{jW_1 t}, \qquad \bar{U}'' = jW_1 \bar{\Psi}''. \tag{1a,b,c}$$

The commutation of MSC converter is dependent on the flux $\bar{\psi}''$ , the voltage $\bar{u}''$ , the subtransient inductance $L''$ and the stator resistance $R$. The MSC converter is only in the $W_1 \geq R/L''$ speed range able to perform with safe commutation. The results of the classical converter theory can be applied if in this so-called machine commutated range the $R$ resistance is neglected and an $i_d = I_d$ smooth direct current ($L_F = \infty$ inductance) is presumed [3]. Calculations are performed in the CFSM machine commutated range in per unit system, presuming a machine having $2p = 2$ poles.

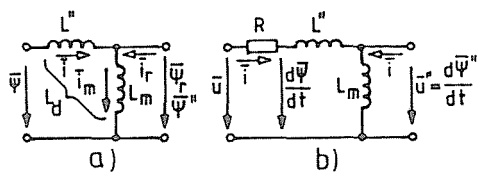


*Fig. 2.* Equivalent circuits of the synchronous machine

## 3. Current Harmonics

Because of the MSC converter, the synchronous machine receives a nonsinusoidal supply. The Park vectors in the standing coordinate system show a six-sided symmetry. Therefore in the synchronous machine harmonics of $\nu = 1 + 6k$ ($k = 0, \pm 1, \pm 2, \ldots$ order, $\nu = \ldots, -11, -5, 1, 7, 13, \ldots$) will be developed. The Park vectors can be expanded into a Fourier series, and thus e.g. the current can be written in the following form:

$$\bar{i} = \bar{I}_1 e^{jW_1 t} + \sum_{\nu \neq 1} \bar{I}_\nu e^{j\nu W_1 t} = \bar{i}_1 + \Delta\bar{i}. \tag{2}$$

In (2) $\bar{i}$ has been separated into two parts: the $\bar{i}_1$ fundamental harmonic and to the $\Delta\bar{i}$ deviation from it. Since $\bar{i}_m = \bar{\psi}''/L_m$ consists only of fundamental harmonics, by the application of the $\bar{i}_m = \bar{i} + \bar{i}_r$ nodal equation

$$\bar{i}_{m1} = \bar{i}_1 + \bar{i}_{r1}, \quad \overline{\Delta i} = -\overline{\Delta i_r} \tag{3a,b}$$

can be obtained.

Applying Park vectors, it is advisable to turn to a coordinate system, which rotates with $W_1$ synchronous speed, as in this case the fundamental harmonics are stationary. If the real axis $x$ of the synchronously rotating coordinate system is fixed to the $\bar{u}''$ induced voltage, then in accordance with the $\bar{i}^* = \bar{i}e^{-jW_1t}$ transformation equation for the stator current, the following equation will be obtained ($\nu - 1 = 6k$):

$$\bar{i}^* = \bar{I}_1 + \sum_{\nu\neq 1} \bar{I}_\nu e^{j(\nu-1)W_1t} = \bar{i}_1^* + \Delta\bar{i}^*. \tag{4a}$$

It can be seen that the frequency of the current harmonics is coordinate system dependent. Besides the frequency, the phase angle of the complex amplitudes of the current harmonics depends on the coordinate system as well. Likewise, if the current vector is written in a $d-q$ coordinate system which is rotating with synchronous speed, then

$$\bar{i}_{dq}^* = \bar{I}_{1dq} + \sum_{\nu\neq 1} \bar{I}_{\nu dq} e^{j(\nu-1)W_1t}, \tag{4b}$$

where $\bar{I}_{\nu dq} = \bar{I}_\nu e^{j(90^\circ+\beta)}$ and $90^\circ + \beta$ is the angle between the $x$ and $d$ axes.

*Fig. 3* shows conditions in a coordinate system rotating with synchronous speed. It can be seen from the figure that the $\alpha$ (or $\alpha_p$) firing angle unambiguously defines the angle of the $\bar{i}^*$ current vector at the instant of firing (in the point $F$). The three phase conduction (overlap) corresponding to the commutation lasts from $F$ to $E$, and from $E$ to $F$ the two phase conduction following the overlap. The latter is positioned on the arc having $60^\circ - \delta$ angle of the circle with the radius of $I_0 = (2/\sqrt{3})I_d$ ($\delta$: overlap angle). At the instant of extinction (in point $E$) the angle of $\bar{i}^*$ will be determined by the $\kappa = \alpha + \delta$ extinction angle. The leaf shaped curve of $\bar{i}^*$ current vector becomes closed with a tact timing of $\tau = \pi/(3W_1)$ and repeats itself with $6f_1$ frequency. The $\bar{I}_1$ fundamental harmonic points to the time weighted center of gravity of the curve. The angular velocity of the harmonics is $(\nu - 1)W_1$ ($\nu - 1 = \cdots -12, -6, 6, 12, \ldots$) according to (4a). The harmonics give in pairs ($\nu - 1 = -6, 6; -12, 12, \ldots$) elliptically shaped paths. From the figure it can be realized that $\Delta^* = 30^\circ - \Delta$ is the angle of

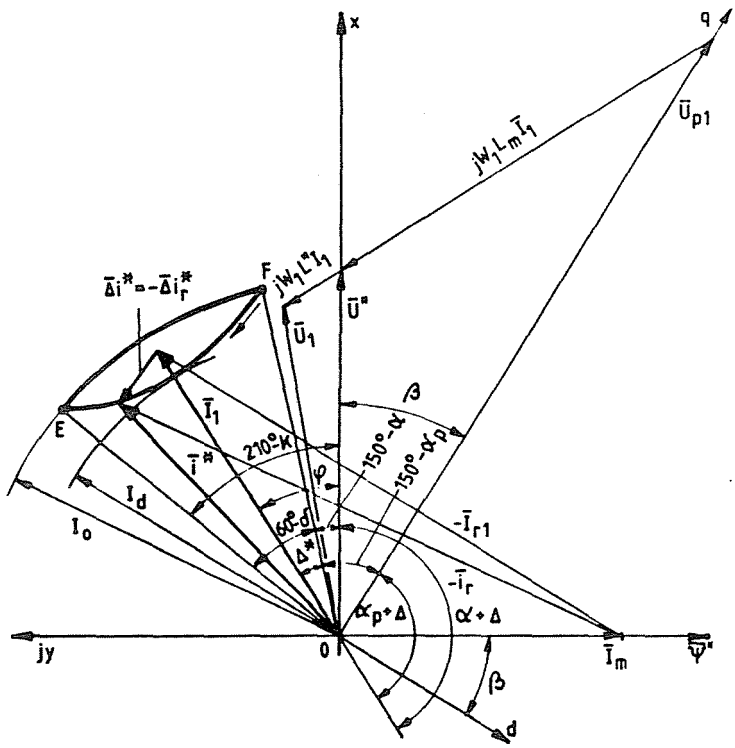


*Fig. 3.* Current vector in the rotating coordinate system

the $\bar{I}_1$ fundamental harmonic measured from the firing point $F$, and thus $\varphi = 180° - (\alpha + \Delta)$ is its phase angle ($\varphi + 90° = \vartheta$ is the torque angle).

Completing the complex expansion into a Fourier series for the $\bar{I}_\nu$ complex amplitude will be obtained

$$\bar{I}_1 = I_s \frac{3}{2\pi}\left[j\delta - j\sin\delta e^{-j(2\alpha+\delta)}\right] = I_1 e^{j\varphi}, \tag{5a}$$

$$\bar{I}_\nu = \frac{3}{\pi}\frac{I_s}{\nu(\nu^2-1)}\Big\{-[\cos(\alpha+\delta) - j\nu\sin(\alpha+\delta)]e^{-j\nu(\alpha+\delta)} - \\ -(\nu\cos\alpha + j\sin\alpha)e^{-j\nu\alpha} + (\nu+1)e^{-j(\nu-1)\alpha}\Big\}, \tag{5b}$$

where $I_s = \Psi''/L''$ is the short circuit current. Knowing the $\alpha(\delta)$ control characteristic based on it, the $\bar{I}_\nu^* = \bar{I}_\nu/I_s$ normalized harmonic current can be determined. The $\nu = -5.7$ harmonic currents belonging to various extinction angles are demonstrated in *Fig. 4a*. ($M$ is the torque,

$M/M_{mi}$ is the normalized torque, $M_{mi} = \Psi'' I_s/2)$. In practice a more useful result will be obtained if the harmonics are related to the $I_1$ fundamental harmonic. *Fig. 4b* shows the $I_\nu/I_1$ harmonic/fundamental harmonic ratio. In the case of $M = 0$ ($\delta = 0$), $I_\nu/I_1 = |1/\nu|$.

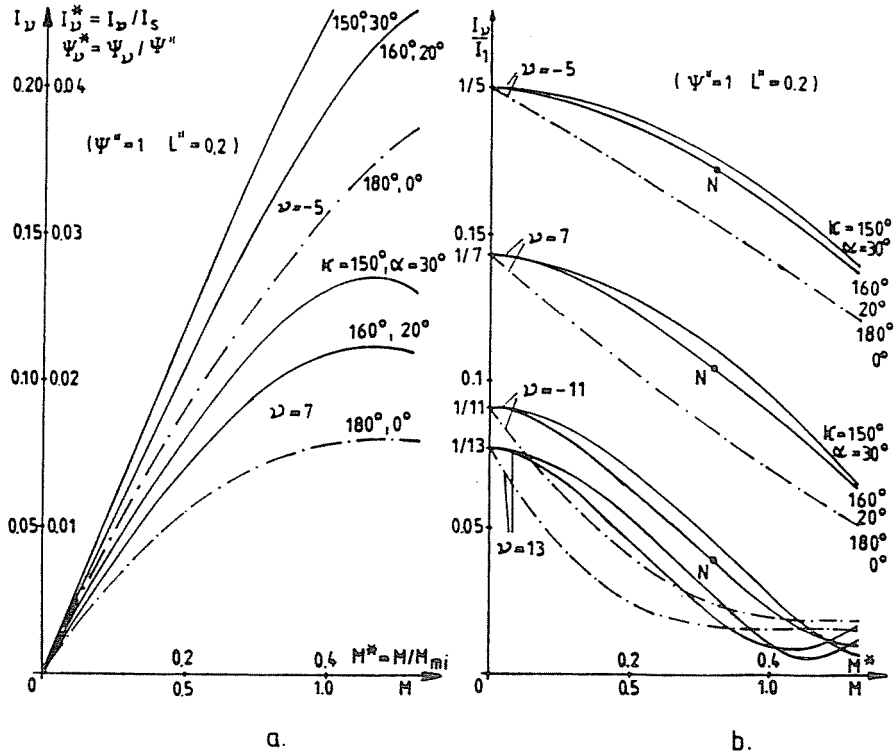


*Fig. 4a, b.* Amplitudes of current harmonics

From the current harmonics, both the flux and the voltage harmonics can be determined:

$$\bar{\Psi}_\nu = L'' \bar{I}_\nu, \qquad \bar{U}_\nu = j\nu W_1 \bar{\Psi}_\nu = j\nu W_1 L'' \bar{I}_\nu. \tag{6a,b}$$

It follows from (6) that $\Psi_\nu^* = \Psi_\nu/\Psi'' = I_\nu^* = I_\nu/I_s = U_\nu^*/|\nu| = U_\nu/|\nu U''|$. From the current harmonics to the additional copper losses, from the voltage harmonics to the additional iron losses can be concluded.

## 4. Additional Copper Losses

Knowing the amplitude values of the current harmonics, the Park vector effective values of the currents can be calculated by an infinite series:

$$\Delta I_{\text{eff}}^2 = \sum_{\nu \neq 1} I_\nu^2 = I_{\text{eff}}^2 - I_1^2, \qquad I_{\text{eff}}^2 = \sum_{\nu=1}^{\infty} I_\nu^2 = I_1^2 + \Delta I_{\text{eff}}^2, \tag{7a,b}$$

$$I_{r\text{eff}}^2 = \sum_{\nu=1}^{\infty} I_{r\nu}^2 = I_{r1}^2 + \Delta I_{\text{eff}}^2 = I_f^2 + \Delta I_{\text{eff}}^2. \tag{7c}$$

Using the six-sided symmetry of the $\bar{i}$ stator current, the vectorial effective value of the stator current can be defined by the definitive equation

$$I_{\text{eff}}^2 = \frac{1}{\tau} \int_{(\tau)} |\bar{i}|^2 dt = \frac{1}{\tau} \int_{(\tau)} \bar{i}\hat{i} dt \tag{8}$$

even in closed form. Carrying out the integration, after the reduction the result will become:

$$I_{\text{eff}}^2 = I_s^2 \left\{ (1 - A)(1 - \cos\delta) - \frac{3}{\pi} \left[ (1 + A + \cos\delta)\frac{\delta}{2} - \right.\right.$$

$$\left.\left. - \left(1 + \frac{A}{2}\right) \sin\delta \right] \right\}, \tag{9}$$

where $A = \cos(2\alpha + \delta)$. Knowing $I_{\text{eff}}^2$ and $I_1^2$, $\Delta I_{\text{eff}}^2$ can be obtained by (7a). In *Fig. 5* the effective values of the currents ($I_{\text{eff}}^2$, $\Delta I_{\text{eff}}^2$ and $I_{r\text{eff}}^2$) are given. Applying the normalized scale (denoted by $*$), according to $I_{\text{eff}}^2 = I_s^2 I_{\text{eff}}^{*2}$ and $\Delta I_{\text{eff}}^2 = I_s^2 \Delta I_{\text{eff}}^{*2}$ they can be defined for any machine data. The $I_{r\text{eff}}^2 = I_s^2 I_{r\text{eff}}^{*2}$ square of the rotor current can be obtained from the figure only by having $L''/L_m = 0, 2/1, 3$ ratio. For the sake of better reading the ten times value of $\Delta I_{\text{eff}}^2$ has been represented.

It follows from (6.a):

$$\Delta\Psi_{\text{eff}} = L'' \Delta I_{\text{eff}}, \tag{10a}$$

$$\Delta\Psi_{\text{eff}}^* = \Delta\Psi_{\text{eff}}/\Psi'' = \Delta I_{\text{eff}}/I_s = \Delta I_{\text{eff}}^*. \tag{10b}$$

The copper losses of both the stator and the rotor can be divided into two parts, to the fundamental harmonic ($\Delta P_1$ and $\Delta P_{r1}$) and harmonic ($\Delta P_\nu$ and $\Delta P_{r\nu}$) losses:

$$\Delta P = I_1^2 R_1 + \sum_{\nu \neq 1} I_\nu^2 R_\nu = \Delta P_1 + \Delta P_\nu, \tag{11a}$$

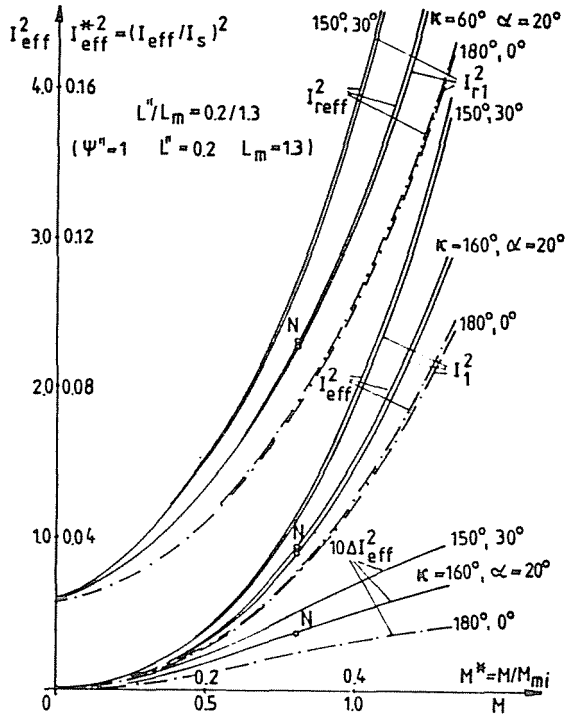


*Fig. 5.* Squares of the effective values of currents

$$\Delta P_r = I_{r1}^2 R_{r1} + \sum_{\nu \neq 1} I_{r\nu}^2 R_{r\nu} = \Delta P_{r1} + \Delta P_{r\nu}. \tag{11b}$$

In the equation $R_1$ is the stator resistance at the $f_1$ fundamental harmonic frequency, while at the $|\nu f_1|$ harmonic frequency it is $R_\nu$; $R_{r1}$ is the d.c. resistance of the rotor, while at $|(\nu-1)f_1|$ harmonic frequency it is $R_{r\nu}$. The influence of the skin effect on $L''$ can be taken into consideration in the approximate calculation by using the $L''$ belonging to $6f_1$. If the skin effect can be neglected ($R_\nu = R = \text{const.}$, $R_{r\nu} = R_r = \text{const.}$), then the effective values of the currents determine the copper losses as well:

$$\Delta P = I_{\text{eff}}^2 R = I_1^2 R + \Delta I_{\text{eff}}^2 R = \Delta P_1 + \Delta P_\nu, \tag{12a}$$

$$\Delta P_r = I_{r\text{eff}}^2 R_r = I_{r1}^2 R_r + \Delta I_{r\text{eff}}^2 R_r = \Delta P_{r1} + \Delta P_{r\nu}. \tag{12b}$$

To make the order of magnitudes perceptible, $I_1^2$ and $I_{r1}^2$ have been drawn in *Fig. 5* as well. It can be seen that in the CFSM the additional copper losses deriving from the nonsinusoidal currents are very small. For example,

in the point denoted by $N$, $I_1 \approx 0.95$, $I_1^2 \approx 0.90$, $I_{r1} \approx 1.51$, $I_{r1}^2 \approx 2.28$, $\Delta I_{\text{eff}}^2 \approx 0.04$. According to (12) the values mean that with resistances $R = R_r = 0.02$, $\Delta P_1 \approx 0.9 \cdot 0.02 = 0.018$, $\Delta P_{r1} \approx 2.28 \cdot 0.2 \approx 0.046$, $\Delta P_\nu = \Delta P_{r\nu} \approx 0.04 \cdot 0.02 \approx 0.001$ copper losses will be obtained (in this same point according to $P_m = MW_1 = 0.8W_1$ mechanical power is a function of the angular velocity). In the sinusoidal rated point $M \approx \cos\varphi_1 = 0.8$, $I_1 = 1.0$, $I_1^2 = 1.0$, $I_{r1} \approx 1.73$, $I_{r1}^2 \approx 3.0$, $\Delta P_n = 1.0 \cdot 0.02 = 0.02$, $\Delta P_{rn} = 3.0 \cdot 0.02 = 0.06$. As in point $N$ $\Delta P < \Delta P_n$ and $\Delta P_r < \Delta P_{rn}$, and thus in spite of the additional copper losses caused by the harmonics the CFSM is able to exert its rated torque even in this point.

The current distortion factor is

$$k_i = \frac{\sum\limits_{\nu \neq 1} I_\nu^2}{I_1^2} = \frac{\Delta I_{\text{eff}}^2}{I_1^2} = \frac{I_{\text{eff}}^2 - I_1^2}{I_1^2}. \tag{13}$$

If there is no skin effect in the stator, then the $k_i = \Delta P_\nu / \Delta P_1$ equation can be obtained; i.e. in such a case this factor is characteristic to the additional stator copper loss as well. *Fig. 6* shows the $k_i$ current distortion factor as a function of the $\delta$ overlap angle. The value of $k_i \approx 0.043$ in point $N$ means that the stator copper loss increases by 4.3 % because of the nonsinusoidal current compared to that of the sinusoidal operation. Neglecting the overlap $(\delta = 0) k_{i0} = (\pi/3)^2 - 1 \approx 0.097$.

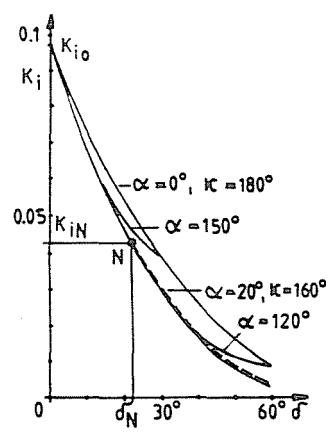


*Fig. 6.* Current distortion factor

It can be seen from the calculation example that neglecting the skin effect, in point $N$ the proportion of the harmonics is 5% out of the stator

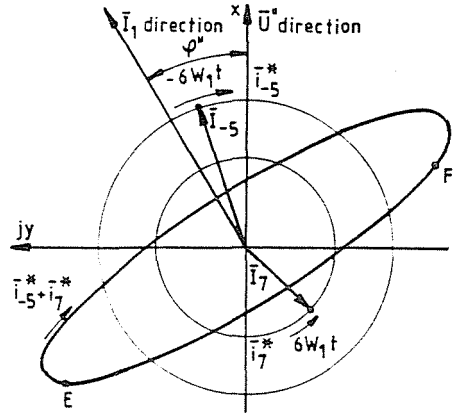


*Fig. 7a.* 5th and 7th current harmonics in rotating coordinate system

copper loss, and it is only 2% out of the rotor copper loss. However, in the rotor the skin effect cannot be neglected (primarily because of the damping cage). The $\Delta P_{r\nu}$ rotor additional copper loss in (11b) may become by one order of magnitude greater as compared to the case without skin effect. Warming up of the rotor increases because the utilization of the damping cage by the harmonics is not circle symmetric , as the component of the harmonic rotor current having $\mu f_1$ frequency ($\mu = |\nu - 1|$) is in the synchronously rotating coordinate system such a current vector which is travelling on an elliptic locus, which shows in the $d$ and $q$ directions various projections. The reason for this is that in the synchronously rotating coordinate system the current harmonics having $\mu f_1 = 6f_1, 12f_1, \ldots$ frequency are composed of positive and negative components. In *Fig. 7a*, for example, the harmonics of the order $\nu = 1 - \mu = -5$ and $\nu = 1 + \mu = 7$ corresponding to $\mu = 6$ are represented individually and as resultants in the synchronously rotating $x - y$ coordinate system.

The currents in the $d - q$ coordinate system can be written in the following form:

$$\bar{i}^*_{dq} = i_d + ji_q = I_{1d} + \Delta i_d + j(I_{1q} + \Delta i_q), \tag{14a}$$

$$\bar{i}^*_{rdq} = i_{rd} + ji_{rq} = I_{r1d} + \Delta i_{rd} + j(I_{r1q} + \Delta i_{rq}), \tag{14b}$$

where $I_{r1d} = I_f$, $I_{r1q} = 0$, $\Delta i_{rd} = -\Delta i_d$, $\Delta i_{rq} = -\Delta i_q$. The harmonics of the order $\nu = 1 + \mu$ and $\nu = 1 - \mu$ are developing $i_{\mu d}$ and $i_{\mu q}$ components of $\mu f_1$ frequency which are contained in the $d$ and $q$ components of the current harmonics, and thus they can be obtained by the projection of the current

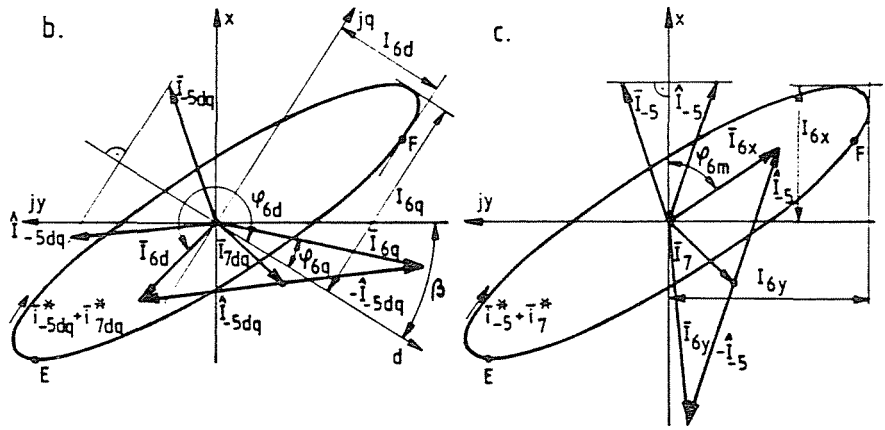


*Fig. 7b,c.* 5th and 7th current harmonics in rotating coordinate system

vector moving along the elliptic locus according to $\bar{i}^*_{(1+\mu)dq} + \bar{i}^*_{(1-\mu)dq}$ onto the $d-q$ axes:

$$i_{\mu d} = Re\left(\bar{i}^*_{(1+\mu)dq} + \bar{i}^*_{(1-\mu)dq}\right) = Re\left(\bar{i}^*_{(1+\mu)dq} + \hat{i}^*_{(1-\mu)dq}\right),$$

$$i_{\mu q} = Im\left(\bar{i}^*_{(1+\mu)dq} + \bar{i}^*_{(1-\mu)dq}\right) = Im\left(\bar{i}^*_{(1+\mu)dq} - \hat{i}^*_{(1-\mu)dq}\right). \qquad (15a,b)$$

The vector $\bar{i}^*_{(1+\mu)dq}$ and $\hat{i}^*_{(1-\mu)dq}$ rotate with $\mu W_1$ angular velocity in the same direction, and thus for the amplitudes the vectorial summation can be applied:

$$\bar{I}_{\mu d} = \bar{I}_{(1+\mu)dq} + \hat{I}_{(1-\mu)dq}, \qquad (16a)$$

$$\bar{I}_{\mu q} = \bar{I}_{(1+\mu)dq} - \hat{I}_{(1-\mu)dq}. \qquad (16b)$$

The component having $f_1$ frequency is of $I_{\mu d} = |\bar{I}_{\mu d}|$ amplitude in the $d$ direction current component and of $I_{\mu q} = |\bar{I}_{\mu q}|$ in the $q$ direction current component. Based on (15, 16)

$$\bar{i}_{\mu d} = Re\left(\bar{I}_{\mu d} e^{j\mu W_1 t}\right) = I_{\mu d}\cos(\mu W_1 t + \varphi_{\mu d}), \qquad (17a)$$

$$\bar{i}_{\mu q} = Im\left(\bar{I}_{\mu d} e^{j\mu W_1 t}\right) = I_{\mu q}\sin(\mu W_1 t + \varphi_{\mu q}), \qquad (17b)$$

where $\varphi_{\mu d} = \mathrm{arc}\,(\bar{I}_{\mu d})$, $\varphi_{\mu q} = \mathrm{arc}\,(\bar{I}_{\mu q})$. *Fig. 7b* shows the amplitudes and angles belonging to $\mu = 6$ for the orders of $\nu = -5$ and 7. The current deviations in the $d$ and $q$ axes can be calculated by the infinite sums of the Fourier series according to:

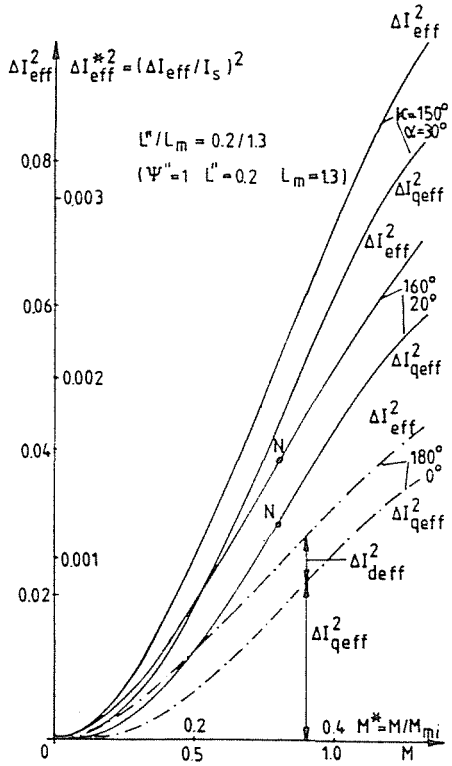


*Fig. 8.* Disintegration of $\Delta I^2_{\text{eff}}$

$$\Delta i_d = \sum_{\mu \neq 0} i_{\mu d}, \qquad \Delta i_q = \sum_{\mu \neq 0} i_{\mu q}. \tag{18a}$$

The effective values of the current deviations in the $d$ and $q$ directions are:

$$\Delta I^2_{d\text{eff}} = \frac{1}{2} \sum_{\mu \neq 0} I^2_{\mu d}, \qquad \Delta I^2_{q\text{eff}} = \frac{1}{2} \sum_{\mu \neq 0} I^2_{\mu q}. \tag{18b}$$

Since the $d$ and $q$ components are perpendicular to each other, the

$$\Delta I^2_{d\text{eff}} + \Delta I^2_{q\text{eff}} = \Delta I^2_{\text{eff}} \tag{19}$$

equality is obviously valid. *Fig. 8* shows the decomposition of $\Delta I^2_{\text{eff}}$ into the direct and quadrature axis. It can be seen that about the rated torque $M \approx 0.8\ \Delta I^2_{q\text{eff}} \gg \Delta I^2_{d\text{eff}}$, so that in point $N$ $\Delta I^2_{q\text{eff}} \approx 0.03$, $\Delta I^2_{d\text{eff}} \approx 0.008$.

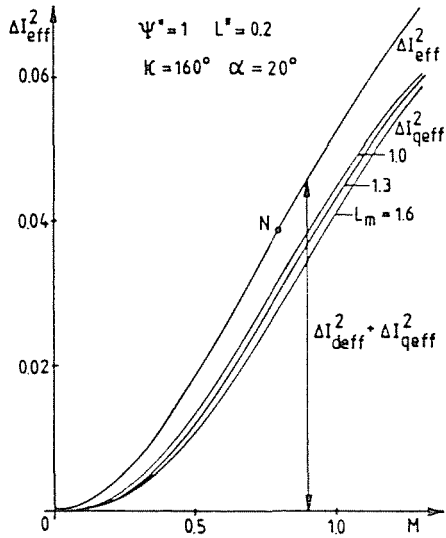


*Fig. 9.* Dependence of $\Delta I^2_{\text{eff}}$ and $\Delta I^2_{q\,\text{eff}}$ on the $L_m$

This means that the harmonics utilize primarily the coil of the $q$ direction if $\kappa = 160°$ (*Fig. 3*). Therefore, the damping cage of the synchronous machine of the CFSM is advised to be designed with the minimum skin effect in the bars next to the axis $d$.

The decomposition of $\Delta I^2_{\text{eff}}$ in the $d-q$ directions depends on the $L''/L_m$ ratio. *Fig. 9* shows the decomposition of $\Delta I^2_{\text{eff}}$ in the $d-q$ directions for various $L_m$ inductances. It can be seen from the $\Delta I^2_{q\,\text{eff}}$ curves that the change of $L_m$, even within a broad range, modifies the decomposition of $\Delta I^2_{\text{eff}}$ only to a small extent.

In *Figs. 4, 5, 6, 8* and *9* the curves belonging to $\kappa =$ constant extinction angle mean at the same time the supplementary angle curves which belong to the $\alpha = 180° - \kappa$ firing angle.

From the investigations carried out follows that from amongst the additional copper losses, the stator loss can in general be neglected, but the rotor loss, because of the skin effect, has to be taken into consideration.

## 5. Additional Iron Losses

The upper harmonics in the fluxes (in the voltages) cause additional iron losses. From the investigations it can be established that the additional iron losses in the CFSM can be neglected.

## 6. Torque Pulsations

The instantaneous value of the torque is:

$$m = \bar{\psi} \times \bar{i} = \bar{\psi}'' \times \bar{i}. \tag{20}$$

The equation with the subtransient flux is the most expedient as $\bar{\psi}''$ consists purely of fundamental harmonic. A particularly simple result is obtained in the synchronous rotating coordinate system:

$$m = \bar{\Psi}'' \times \bar{i}^* = \Psi'' Re(\bar{i}^*). \tag{21}$$

The $\bar{i}^*$ current disintegrates to the $\bar{i}_1^* = \bar{I}_1$ fundamental harmonic and to the $\Delta\bar{i}^*$ deviation, according to $m = M + \Delta m$, and the torque disintegrates to the $M$ mean value and the $\Delta m$ pulsation as well:

$$M = \Psi'' Re(\bar{I}_1), \qquad \Delta m = \Psi'' Re(\Delta\bar{i}^*). \tag{22a,b}$$

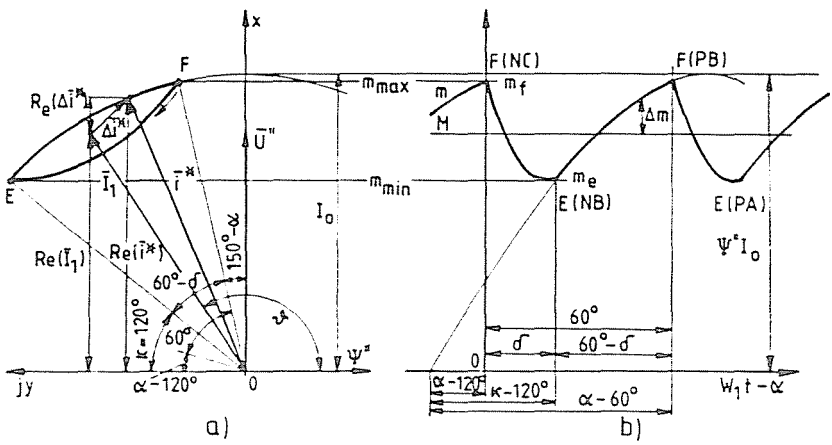


*Fig. 10.* Current vector $\bar{i}^*$ and torque $m$.

In *Fig. 10a* in the $x - y$ coordinate system current vector $\bar{i}^* = \bar{I}_1 + \Delta\bar{i}^*$ is given again; in *Fig. 10b*, however, the torque is calculated on the basis of (21, 22). The torque $m(t)$ repeats itself at every 1/6 period with $6f_1$ frequency similarly to $\bar{i}^*(t)$, and accordingly it has components of $\mu f_1$ frequency ($\mu = 0$ denotes the mean value, $\mu = 6, 12 \ldots$ the pulsations). It can be seen from the figure that in the section where there is no overlap, the

torque travels on a $60° - \delta$ section of a sine curve of $\Psi'' I_0$ amplitude. It can be seen that the $\alpha$ firing angle determines the torque in the point $F$ of firing, however, the $\kappa$ extinction angle determines the torque in the point $E$ of extinction: $m_f = \Psi'' I_0 \sin(\alpha - 60°)$, $m_e = \Psi'' I_0 \sin(\kappa - 120°)$. In the figure at the same time $m_f$ is the maximum and $m_e$ is the minimum torque. In the point $N$, $M = 0.8$, $m_{\max} = m_f \approx 0.98$ and $m_{\min} = m_e \approx 0.64$ will be obtained, and thus the resultant amplitude of the torque pulsation is $\Delta M = (m_{\max} - m_{\min})/(2M) = (0.98 - 0.64)/1.6 \approx 0.21$. From *Fig. 10* reveals that near the extinction limit ($\kappa = 180°$) $m_{\max} = \Psi'' I_0 > m_f$, $m_{\min} < m_e$.

The periodically varying torque can be expanded into a Fourier - series:

$$m(t) = \sum_{\mu=0}^{\infty} M_\mu \cos(\mu W_1 t + \varphi_{\mu m}). \tag{23}$$

The $\mu$th (e.g. 6th) harmonic of the torque is caused by the $\nu = 1 - \mu$ and $1 + \mu$ (e.g. $-5$ and 7) current harmonics which in pairs form an ellipse. By the application of (22b) for the two current components, for the instantaneous value the equation

$$m_\mu = \Psi'' Re(\bar{i}^*_{1+\mu} + \hat{i}^*_{1-\mu}), \tag{24}$$

and for the amplitude and the phase angle

$$M_\mu = \Psi'' I_{\mu x}, \qquad \varphi_{\mu m} = \operatorname{arc}(\bar{I}_{\mu x}) \tag{25}$$

are obtained. Here $I_{\mu x} = |\bar{I}_{\mu x}| = |\bar{I}_{1+\mu} + \hat{I}_{1-\mu}|$ is the amplitude of the $x$ direction component of the ellipse consisting of the current harmonics of the order of $1 + \mu$ and $1 - \mu$. These equations are similar in their structure to equations $i_{\mu d}$ and $I_{\mu d}$ (15a) and of (16a). In *Fig. 7c* the $\bar{I}_{6x} = \bar{I}_7 + \hat{I}_{-5}$ (and the $\bar{I}_{6y} = \bar{I}_7 - \hat{I}_{-5}$) current amplitude and the $\varphi_{6m}$ angle are shown for $\mu = 6$ (for $\nu = -5$ and 7).

*Fig. 11* shows the $M_6/M$ and $M_{12}/M$ amplitudes of the $\mu = 6$th and 12th torque upper harmonics related to the mean value. In point $N$, $M_6/M \approx 0.19$ and $M_{12}/M \approx 0.045$ will be obtained ($M_6 \approx 0.19 \cdot 0.8 = 0.152$, $M_{12} \approx 0.045 \cdot 0.8 = 0.036$). It can be seen that especially the amplitude of the component having $6f_1$ frequency is very significant. In general purpose drives which operate in the $f_1 = 5$ Hz range, the pulsation of the torque does not cause any problem in spite of the large $M_6$ amplitude.

## 7. The 12 Pulse CFSM

The pulse number can be increased at good motor utilization only with special connections. Such is the series connection solution shown in *Fig. 12*

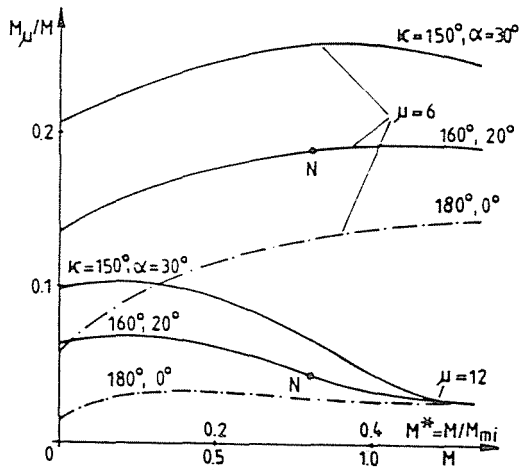


*Fig. 11.* Harmonics of the torque

which contains two stator windings and two converters. If the I and II coil systems are shifted in the space by 30° and the MSCI and MSCII converters are controlled similarly with a 30° shift in time, the a CFSM having 12 pulses will be obtained.

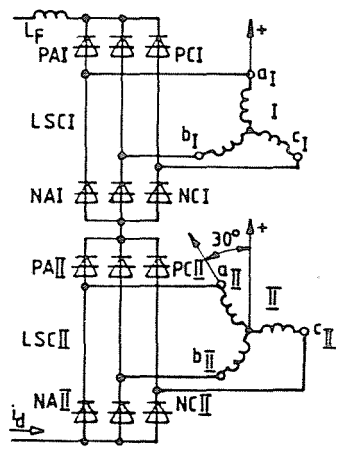


*Fig. 12.* 12 pulse CFSM with double star winding

In *Fig. 13a, b* and *c* the equivalent circuits of the synchronous machines are shown which possess two coils shifted in the space. In *Fig. 13b* and *13c* the rotor number of turns is referred to the stator. The leakage inductances

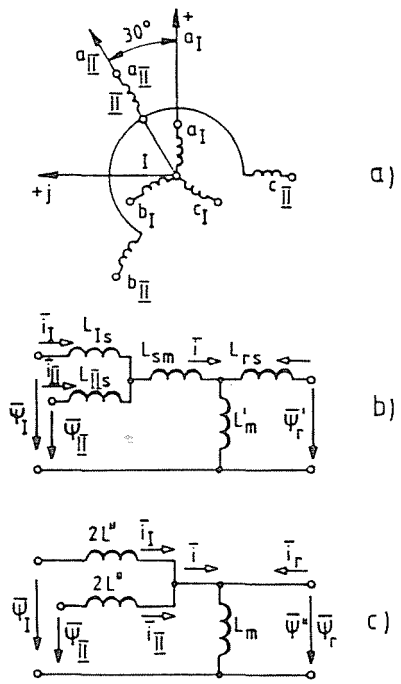


*Fig. 13.* Equivalent circuits of the double star $SM$

of the stator $L_{Is}$ and $L_{IIs}$ takes into consideration the proper leakage of the two coils, however, $L_{sm}$ considers that of the common leakage of the two coils. The *Fig. 13c* becomes true only if for the stator leakages the $L_{sm} = 0$ and the $L_{Is} = L_{IIs} = L_s$ equalities are valid.

Were the two coil systems unidirectional, then $\bar{\psi}_I = \bar{\psi}_{II} = \bar{\psi}$ and $\bar{i}_I = \bar{i}_{II} = \bar{i}/2$. Connecting the coils of the same direction into series, then with the equivalent circuit shown in *Fig. 2a* the synchronous machine of the 6 pulse CFSM would be obtained. The Park vectors having $I$ subscript ($\bar{\psi}_I$ and $\bar{i}_I$) refer to the coil system $I$, and the ones having $II$ subscript to the coil system $II$ and are formed in their own ($a_I, b_I, c_I$ and $a_{II}, b_{II}, c_{II}$ respectively) coordinate system from the phase quantities according to their definition. In the common coordinate system according to *Fig. 13c* the same $\bar{\psi}''$ subtransient flux is connected to both of the stator windings, and thus the $\bar{u}''$ induced voltages are equal as well.

The two converters commutate separately from each other because of the approximation based on the constancy of the subtransient flux. In their proper coordinate system both the $\bar{i}_I$ and $\bar{i}_{II}$ currents change according to

the $\bar{i}$ current vector calculated with $2L''$ of the 6 pulse CFSM. Observing from a common coordinate system, according to the shifting of the coils in space by 30° and the firing control in time by 30°, between both $\bar{i}_I$ and $\bar{i}_{II}$ currents there is an angle difference of 30° both in space and time, at the positive direction of rotation:

$$\bar{i}_{II}(W_1 t) = \bar{i}_I(W_1 t - \pi/6)e^{j\pi/6}. \tag{26}$$

The resultant current vector which is proportional to the spatial excitation of the stator can be obtained by the $\bar{i} = \bar{i}_I + \bar{i}_{II}$ summation. The $\bar{i}_I$, $\bar{i}_{II}$ and $\bar{i}$ current vectors are shown in *Fig. 14* (presuming $\delta < 30°$ overlap). The tacts which begin with the firing of the NCI and NCII thyristors are made thicker, and the marks of the conducting thyristors are entered as well.

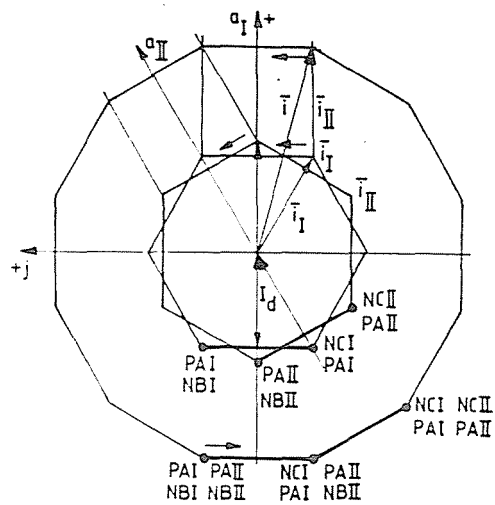


*Fig. 14.* Current vector of the 12 pulse CFSM

For the numerical calculations the $\bar{i}_I$ and $\bar{i}_{II}$ currents were expanded into a Fourier series according to (2). The $\bar{I}_{I\nu}$ and $\bar{I}_{II\nu}$ current amplitudes obtained in their proper coordinate system are equal to the amplitudes calculated with the $2L''$ of the 6 pulse CFSM. From (26) follows that in the common coordinate system there is an $\bar{I}_{II\nu} = \bar{I}_{I\nu}e^{j(1-\nu)\pi/6} = \bar{I}_{I\nu}e^{-jk\pi}$ relationship between the amplitudes ($\nu = 1+6k$). Taking this into account, at the summation of $\bar{i} = \bar{i}_I + \bar{i}_{II}$

$$\bar{I}_\nu = \bar{I}_{I\nu} + \bar{I}_{II\nu} = (1 + e^{-jk\pi})\bar{I}_{I\nu} \tag{27}$$

will be obtained. It follows from the $(1 + e^{-jk\pi})$ multiplication factor that the $\bar{I}_\nu$ amplitude of the resultant of the current harmonics belonging to the zero and even number values of $k$ is twice as much as the $\bar{I}_{I\nu}$ amplitude obtained for coil $I$. This kind is the $\bar{I}_{I1} = \bar{I}_{II1}$ fundamental harmonics ($k = 0, \nu = 1$) and are part of the harmonics ($k = \pm 2, \pm 4, \ldots, \nu = -11, 13, -23, 25, \ldots$). These harmonics of the resultant stator current correspond to the values of the 6 pulse CFSM calculated with $L''$. The harmonics belonging to $k = \pm 1, \pm 3, \ldots (\nu = -5, 7, -17, 19, \ldots)$ drop out of the resultant current vector. This is in accordance with the phenomenon that the $\bar{i}$ resultant current vector seen in *Fig. 14* in consequence of the 12 sided symmetry, can have only harmonics of the order $\nu = 1 + 12k$ ($k = 0, \pm 1, \pm 2, \ldots$). Thus the name 12 pulse CFSM is derived for *Fig. 12.*

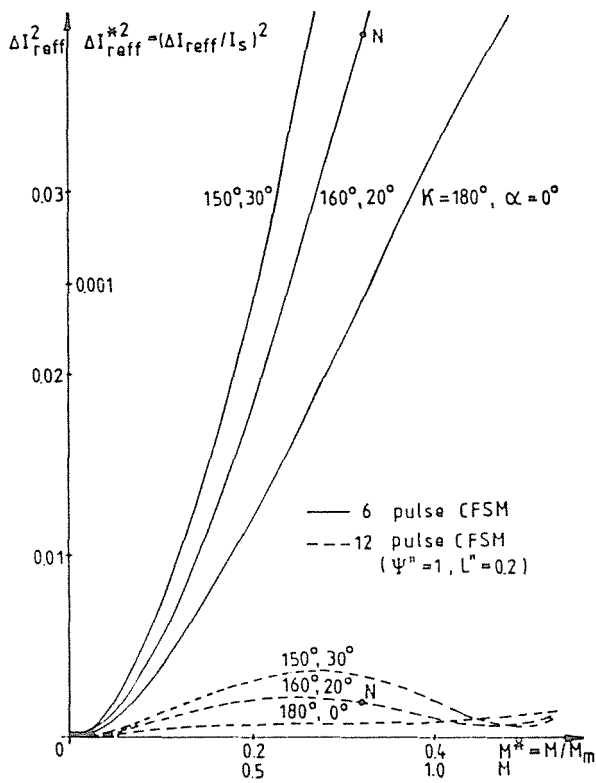


*Fig. 15.* $\Delta I^2_{reff}$ in the 6 and 12 pulse case

From what has been discussed until now can be established that while in the individual stator windings harmonic currents of $\nu = 1 + 6k$ are

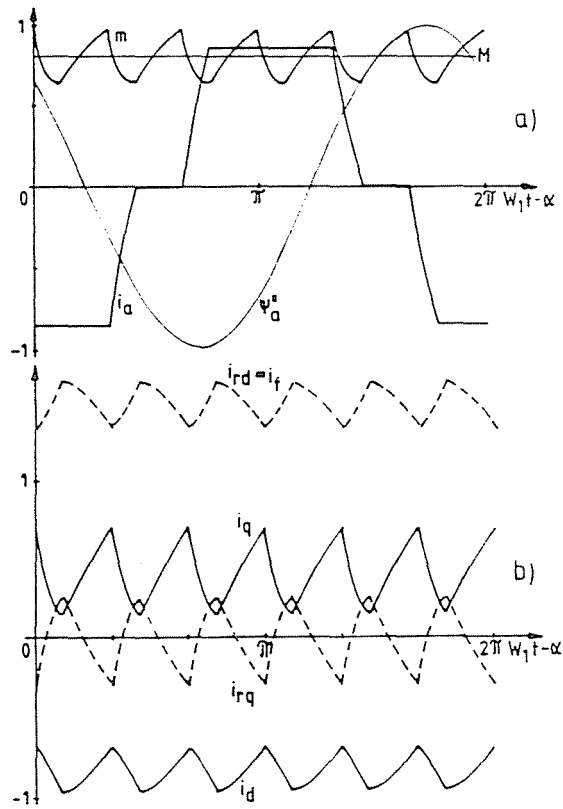


*Fig. 16.* Time functions in the 6 pulse system, rated point

flowing, in the resultant m.m.f. of the stator only the harmonics of $\nu = 1 + 12k$ order are present. From the point of view of the effect on the rotor, the $\bar{i}$ resultant current is authoritative. Thus in the rotor $\Delta\bar{i}_r = \Delta\bar{i} = -(\Delta\bar{i}_I + \Delta\bar{i}_{II})$, i.e. harmonic currents of $\nu = 1 + 12k$ order are flowing ($k = -1, -2, \dots$). It follows from the (22a) torque equation that, from the point of view of the $M$ mean value, the utilization of the 12 pulse CFSM with double winding is as good as that of the 6 pulse one, since the fundamental harmonic m.m.f.-s of the windings are added up algebraically. At the 12 pulse circuit in the $\Delta\bar{i}^-$ current deviation of the synchronously rotating coordinate system and thus in the $\Delta m$ torque pulsation of (22b) as well, there are only components having $\mu f_1 = 12kf_1$ frequency ($k = 1, 2, \dots$). The $M_\mu/M$ relative amplitudes – because of the mathematical summation of the $\bar{I}_{I\nu}$ and $\bar{I}_{II\nu}$ current harmonics having $\nu = 1 + 12k$ order

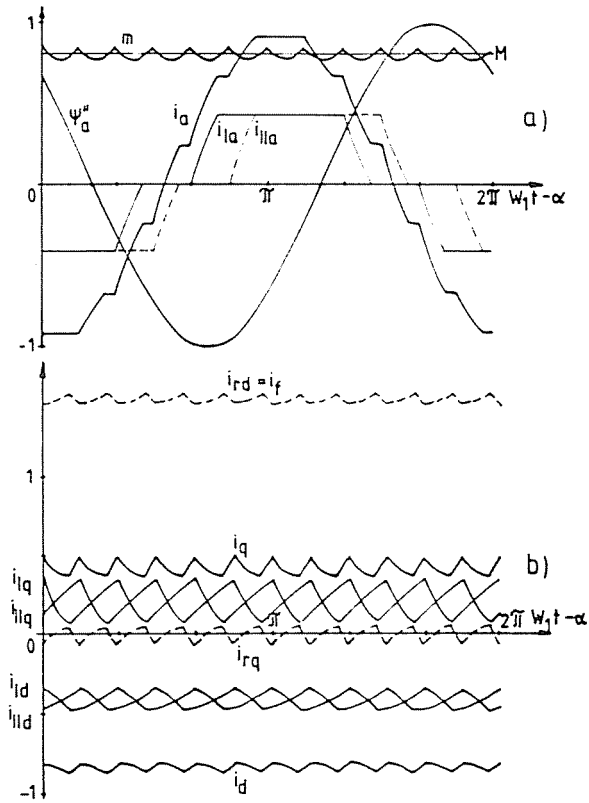


*Fig. 17.* Time functions in the 12 pulse system, rated point

of harmonics – correspond to the amplitudes of the 6 pulse circuit having the same order of harmonics.

It follows from what has been detailed above that certain harmonic characteristics of the 12 pulse circuit can be read from the 6 pulse figures discussed. From *Fig. 4b* the $I_\nu/I_1$ ratio in the stator winding can be obtained. From *Fig. 5* the $\Delta I^2_{\text{eff}}$ characteristic of the additional loss developed in the stator winding can be read. From the current harmonics which can be determined from *Fig. 4b*, $I_{-11}$ and $I_{13}$ flow through the rotor as well. In *Fig. 15* the $\Delta I^2_{\text{eff}} = \Delta I^2_{r\text{eff}}$ of the resultant current deviation of the 12 pulse CFSM is given. This is characteristic of the additional winding loss developed in the rotor of the 12 pulse CFSM. In the same figure the $\Delta I^2_{r\text{eff}}$ curves of the 6 pulse circuit were sketched again. Comparing them, it can be seen that in the 12 pulse circuit $\Delta I^2_{r\text{eff}}$ significantly decreases compared to the 6 pulse circuit (e.g. the measure of decrease in point $N$ is cca 1 : 20 as $\Delta I^2_{r\text{eff}}$

changes from 0.039 to 0.0018). This results in the fact that in such a case the additional winding loss developed in the rotor can be neglected even at significant skin effect. From *Fig. 11* the $M_{12}/M$ ratio can be determined. For example, the amplitude of the torque pulsation having the smallest frequency will decrease in the proportion of $M_{12}/M_6 - 0.045/0.19 - 1/4$ in point $N$ if instead of the 6 pulse circuit, a 12 pulse circuit is applied.

It can be stated that the 12 pulse CFSM having a double winding is equivalent to a 6 pulse CFSM on the basis of the mean values and the stator harmonic currents. In respect of the rotor harmonic currents and that of the torque pulsations it behaves like a 12 pulse circuit.

In order to demonstrate the differences between the 6 pulse and the 12 pulse CFSM circuit, in *Figs. 16, 17* the time functions of $N$ motor point, respectively, are shown. The starting points of the time functions correspond to the firing of the NCI thyristor. In the $\Delta m$ torque pulsation and the $i_{rd}$, $i_{rq}$ rotor current, respectively, the advantageous properties of the 12 pulse circuit can be clearly seen. For instance, the resultant amplitude of the torque pulsation has decreased from the 6 pulse $\Delta M - 0.21$ to $\Delta M - 0.05$ in the 12 pulse operation. The $i_a = Re(\bar{i})$ component is in the 12 pulse circuit merely a fictitious current.

It is advisable to apply the 12 pulse double winding CFSM at large power requirements when the division of the stator winding and MSC converter is necessary anyway.

## References

1. LÜTKENHAUS, H.J. (1975): Drehmoment-Oberschwingungen bei Stromrichtermotoren. *AEG-MITT.* pp. 201–204.
2. CEROVSKY, Z. (1982): Käfigströme und Käfigverluste der Stromrichtermotoren. *Archiv für Elektrotechnik.* pp. 341–348.
3. LÁZÁR, J. (1987): Park-Vector Theory of Line-Commutated Three-Phase Bridge Converters. OMIKK Publisher, Budapest.
4. SCHMIDT, I. (1987): Self Control Methods of the Converter-Fed Synchronous Motor. *Archiv für Elektrotechnik* pp. 11–22.
5. GALASSO, G. (1988): Adjustable Speed Synchronous Motors for Gas Compressors of Falconara Plant. *ICEM Conf.*, Pisa, Appendix, pp. 29–34.